

# How Micro/Nanoarchitecture Facilitates Anti-Wetting: An Elegant Hierarchical Design on the Termite Wing

Gregory S. Watson,<sup>†,\*</sup> Bronwen W. Cribb,<sup>‡</sup> and Jolanta A. Watson<sup>†,§</sup>

<sup>†</sup>School of Pharmacy and Molecular Sciences, James Cook University, Townsville, QLD 4811, Australia, <sup>‡</sup>Centre for Microscopy & Microanalysis and School of Biological Sciences, University of Queensland, St. Lucia, QLD 4072, Australia, and <sup>§</sup>School of Engineering and Physical Sciences, James Cook University, Townsville, QLD 4811, Australia

The purposeful design of surfaces with anti-wetting properties is an increasingly important aspect for new materials and devices. For example, superhydrophobic surfaces are useful for a wide range of applications, from smart microfluidic and lab-on-a-chip devices to large-scale applications, anti-fouling coatings, drag reduction, and oil/water separation.<sup>1–3</sup> Naturally occurring nanostructures are a much-neglected, but potentially rich, source of products exhibiting finely tuned functional efficiencies. While the pharmaceutical industry has long recognized the value of natural compounds, the emerging industries based on nanotechnology have so far made relatively little use of “free” and abundant technology that has been “invented” by the imperatives of species survival. One of the most noteworthy naturally occurring nanocomposite materials is the insect cuticle.<sup>4</sup> Recently, natural micro- and nanostructures found on insect cuticle have been shown to exhibit a range of impressive properties such as superhydrophobicity, self-cleaning technologies, and directed wetting.<sup>4–9</sup> Of notoriety is the water strider, which has thousands of small needle-like projections (setae) which is claimed to hold trapped air, allowing the insect to walk on water.<sup>1,7</sup>

Many terrestrial insects have non-wetting surfaces to contend with the risks associated with living in an environment which offers little protection against wetting by rain and other water surfaces the insect may encounter.<sup>4,5</sup> Thus, there is an evolutionary payoff for such insects to adopt hydrophobic technologies, especially on large surface areas such as the wings. Indeed, insects with a high ratio of wing surface area/body mass (SA/M) or which have a

**ABSTRACT** The termite is an insect which is a weak flier, has a large wing area in relation to its body mass, and many species typically fly during rain or storm periods. Water droplets placed on these insects' wings will spontaneously roll off the surface. Here we show how the intricate hierarchical array design of these insect wings achieves anti-wetting properties with water bodies of various sizes by reducing contact area and thus adhesion. To repel large droplets, the termite uses an array of hairs with a specially designed nanoarchitecture, which we demonstrate is *critical* for this function. By coating single hairs with a polymer of varying thicknesses (with a similar hydrophobicity to insect cuticle), we demonstrate that hairs of the same chemistry and with the complete nanoarchitecture show the greatest resistance to penetrating water bodies. The wings also consist of an underlying non-wetting membrane substructure comprising an array of star-shaped microstructures which minimize interaction with micro-sized droplets of water. The sophisticated micro/nanostructured hierarchy on the termite wing membrane not only results in non-wetting at different length scales but also demonstrates a design for weight and material minimization while achieving this state. Elucidating the function of such structures has implications for understanding insect biology and the evolution of wings.

**KEYWORDS:** termite · insect · micro/nanostructures · atomic force microscopy · anti-wetting · superhydrophobic

close relationship with water generally have water-resistant wings as they are more susceptible to the detrimental adhesional contacts. In the worst case scenario, the insect can become a victim of permanent immobilization on water or wetted surfaces with a reduced capacity to evade or fight off predators. Insects with the above features will typically utilize hydrophobic chemistry and reduce the contact area between insect cuticle and the wetting surfaces with topographical structuring.<sup>4,5</sup> The damselflies, for example, have many thousands of small stalk-like protuberances on the wing membrane which are waxy in nature.<sup>7</sup> Typically, these types of cuticular structures are multifunctional.<sup>10,11</sup> For example, in the case of some cicada, the nanoarchitecture of the wing membrane serves as an anti-reflective surface and also acts as an ultra-low adhesion barrier to contaminating particles and water.<sup>10</sup>

\*Address correspondence to gregory.watson1@jcu.edu.au.

Received for review July 27, 2009 and accepted January 05, 2010.

Published online January 26, 2010. 10.1021/nn900869b

© 2010 American Chemical Society

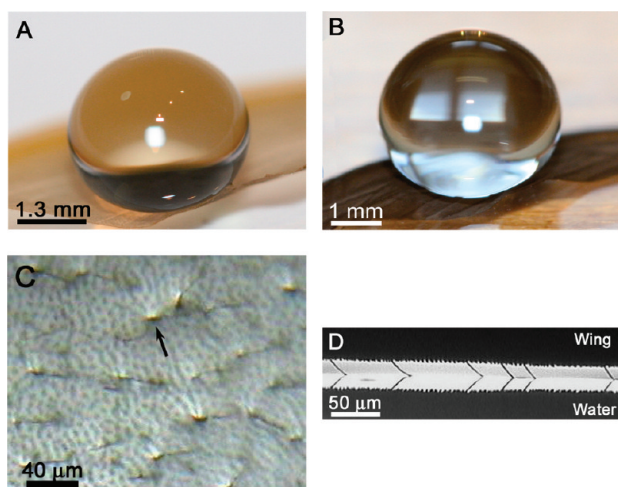


**Figure 1.** (A,B) Optical images showing suspension of water droplets above the wing surface membranes (A) *Nasutitermes* sp. and (B) *Microcerotermes* sp. (C) Optical microscope image (viewing through the droplet from above shown in A) of a water droplet being held up by the hairs (macrotrichia) from the membrane wing surface on *Nasutitermes* sp. (near center of droplet). Not all of the wing hairs directly beneath the water droplet are in contact. The dimpling effect resulting from the indentation of the water surface by the hairs is evident (one example highlighted by the arrow). The hairs are inclined with the surface at slightly different angles. (D) Optical microscope image of *Microcerotermes* sp. resting on bulk water (water bath) showing some of the wing membrane hairs aiding in supporting the insect weight ( $1.84 \times 10^{-3}$  g). The insect was placed wing side down onto the water surface.

Termites (previously Order Isoptera<sup>12</sup>) have an extremely high SA/M value in relation to many other insect species and typically fly from the nest during rain periods.<sup>13</sup> These two features together with the fact that

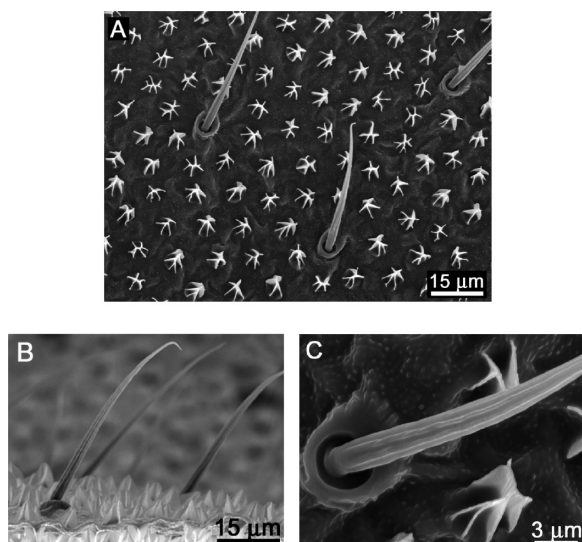


**Figure 2.** SEM images of the termite wing membrane surface *Nasutitermes walkeri*. (A) Topographical landscape showing hairs in sockets (macrotrichia) and star-shaped structures (micrasters) evenly spaced on the surface. (B) Topography (side view) hairs and micrasters on the wing membrane. (C) Higher resolution image showing the hair and micraster fine structure. The hair and micrasters both exhibit a sheet-like structuring. The result is a series of troughs aligned along the long axis on the hairs, while the micrasters exhibit an open framework with radiating arms.

termites are typically very weak fliers indicate that the insect may have specialized hydrophobic structures on its wings. This would optimize the chances of the colonization flight which, even though is generally of a short duration and distance, is critical in the establishment of new colonies.<sup>14</sup> Flying during rain periods may have certain advantages for the insect such as decreasing the likelihood of predator attack due to a mobile canvas of moving droplets. As well, local precipitation will ensure water will be present when establishing a new colony after the initial flight. Water is essential for building nests and soil tunnels, and nest-founding reproductive termites that use soil look for moist soil in which to burrow.<sup>15</sup>

## RESULTS AND DISCUSSION

Optical photography demonstrating the interaction of small droplets of water with the wing membrane on two different termites (*Nasutitermes* sp. and *Microcerotermes* sp.) is shown in Figure 1A,B, respectively. The droplets exhibit remarkable apparent contact angles (CA) of  $180^\circ$  with the underlying membrane.

Without observing the images in Figure 1A,B at higher magnification, one would assume that the water droplets are in “full” direct contact with the wing membrane at various locations. Figure 1C, however, clearly demonstrates that, with the aid of optical imaging through the droplet shown in Figure 1A (*i.e.*, directly from above), many membrane hairs (macrotrichia) support the droplet weight. The contact of hairs with water in the image shows a dimpling effect which is a result of indentation of the water surface by the hairs without penetration of the droplet. Further illustration of this effect is shown in Figure 1D, where a termite wing (still attached to an intact termite, *Microcerotermes* sp.) is “levitating” on bulk water (water bath). The hairs once again protect the wing membrane from coming into contact with the water. As with other insect cuticular structures, hairs on insects have been shown to serve multifunctional purposes such as protection against wetting, minimizing contact with solid surfaces, and in some cases have been attributed to aerodynamic factors.<sup>16–18</sup>

A termite wing that is anchored at one end will quickly shed water droplets off the surface (see Supporting Information videos 1 and 2). Even if an isolated wing is laid on a flat supporting surface (as those shown in Figure 1A,B), it is extremely difficult to place a stable water droplet without artificially creating a region of lower potential energy (*i.e.*, create a well/dip in the middle of the wing membrane allowing the droplet to reach a temporary state of equilibrium). These highly unstable droplets are readily mobilized laterally with a rolling motion along the surface by minor vibrations or inclination of the surface by a few degrees. The anisotropic forces exerted by the hairs (Figure 1C) seem to be one of the contributing factors for the spontaneous re-

removal of water from the termite wing. It is clear that the water droplets in Figure 1A,B encounter a series of hairs/springs with a restoring force balancing the weight of the droplet. To a first approximation for small droplets where contact with the water is very small in relation to the hair length this will simply be

$$F_{\text{drop}} = \sum k\Delta z \quad (1)$$

where  $k$  is the average hair spring constant and  $\Delta z$  the deflection of the hair.

The arrangement of the hairs on the termite membrane is shown in Figure 2A,B. As well, an array of star-shaped structures (micrasters (refer to ref 19)) is clearly seen on the membrane surface, the function and properties of which are discussed in greater detail below. The finer structure of a termite hair is shown in Figure 2C. The hair has a number of open troughs running along the long axis of the shaft. Both termite species examined had this general arrangement where the macrotrichia consisted of a number of open sheeted ridges (50–150 nm radius of curvature), resulting in troughs extending from the hair base to near the hair tip (see also Figure S1 in the Supporting Information). The presence of channels running along the length of the hair is also evident with some semiaquatic insects such as the water strider, which has many thousands of hairs (setae) on each leg. It has been suggested by using the Cassie–Baxter model for wettability that these nanochannels aid in the ability of the legs to resist penetration into the water surface.<sup>8,20</sup>

To investigate whether the hairs' fine structured troughs aided in their ability to resist water penetration, individual termite hair fibers were coated with a hydrophobic polymer (polydimethylsiloxane) (PDMS) (see the Experimental Section for details). This polymer has a measured contact angle with water of  $\sim 105^\circ$ .<sup>1</sup> This represents the upper limit of what can be achieved by nature by virtue of chemistry alone. For example, the cuticle wax on a water strider leg is  $\sim 105^\circ$ .<sup>8,20</sup> Figure 3A reveals the topography and open architecture of an uncoated (*Nasutitermes* sp.) hair in a high-resolution SEM image. The individual termite hairs were then coated with a thin coat of PDMS. The SEM image of a termite hair in Figure 3B shows that, after one thin polymer coat, the open trough structure is reduced but still prominent, still resembling the uncoated hair. A thicker coating removed almost all topographical roughness to the nanoscale and shows no trace of the original topography or evidence of troughs (Figure 3C). Figure 3D,E shows an uncoated and fully coated termite hair shaft demonstrating full coverage of polymer.

The interaction of individual hairs (uncoated and coated) with water (Milli-Q) droplets showed that neither uncoated nor thinly coated hairs penetrated the water droplets at force loadings up to 1.6  $\mu\text{N}$  (Fig-

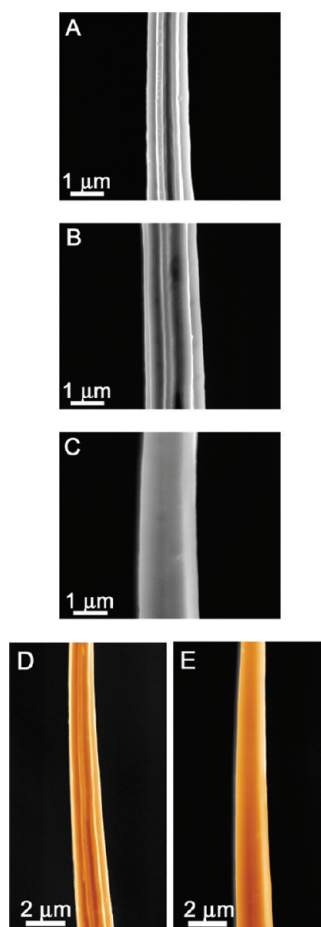


**Figure 3.** (A) High-resolution SEM image revealing the topography and open architecture of an uncoated (*Nasutitermes walkeri*) hair. A significant amount of the original topography (troughs) remains visible on the hair shafts hair after they have been modified by a thin application of PDMS polymer coating (B). After a thicker PDMS coat has been applied, none of the original channel topography is evident (C). Lower resolution image of an uncoated and fully coated termite hair is shown in panels D and E, respectively, demonstrating full coverage by the polymer.

ure 4A,B, respectively). Coated hairs did, however, penetrate the water droplets (Figure 4C).

The mechanical properties of coated and uncoated hairs were determined by deflection with a calibrated atomic force microscope (AFM) lever. The spring/force constants of the coated hairs ( $0.175 \pm 0.023 \text{ N m}^{-1}$  for the thin coat and  $0.185 \pm 0.027 \text{ N m}^{-1}$  for the thick coat) were in the same range as uncoated hairs ( $0.172 \pm 0.030 \text{ N m}^{-1}$ ), which did not penetrate water (for measurements carried out  $10 \pm 2 \mu\text{m}$  from the hair tip (unanchored terminal end)).

When a loading force is applied to the droplets shown in Figure 1A,B (e.g., by microsyringe pressure), the droplet is forced to move closer to the membrane surface; however, when the loading force is removed, the hair arrays spring back and return the droplet to the original position above the surface. The density of hairs on the termite wing can be as high as 5 per  $100 \mu\text{m}^2$ , yielding many thousands of hairs per single wing sur-

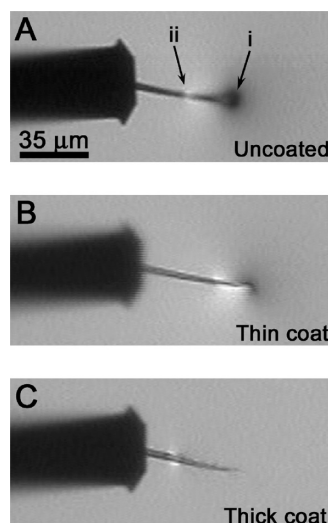


**Figure 4.** (A) Optical images showing the response of individual termite (*Nasutitermes walkeri*) hairs to bulk water solutions, applied maximal loading forces of  $1.37 \pm 0.2 \mu\text{N}$ . The uncoated hair (A) and thin coated hair (B) afford a high resistance to water penetration. The hairs which have their trough topography removed by addition of a thicker polymer coating (C) penetrated into the water.

face. Thus, even for minor hair deflections of less than  $10 \mu\text{m}$ , as little as 100 hairs can easily support the weight of a  $10 \mu\text{L}$  droplet.

AFM adhesion measurements calculated from the snap-on (jump-to-contact) forces were carried out on uncoated and coated hairs with a  $10 \mu\text{L}$  droplet of water. The results showed that uncoated and thin coated hairs yielded adhesion values of (15 and 45 nN, respectively), while thick coated hairs, with no residual channel topography, showed an initial snap-on force of ca. 300 nN.

The results from interacting individually coated and uncoated hairs with droplets shed light on the importance of the micro/nanostructuring in repelling water from the wing surface (Figures 3 and 4). The hairs which were covered with a thin coating of PDMS still retained a significant amount of the topographical structure

(troughs). These “thin coated” hairs, like the uncoated hairs, did not penetrate the water surface under load. “Thick” coated hairs where the topographical fine structure component was removed resulting in a smooth cylinder did, however, penetrate the water surface. Moreover, the spring constants of the coated hairs did not alter enough to account for hair penetration. This clearly demonstrates that the micro/nanoroughness consisting of the open architecture of ridges with troughs is responsible for this effect as the chemistry is maintained (for thin and thick coats) and only the topographical component is altered. The higher adhesion values measured of thick coated hairs in comparison to thinly coated samples also support the previous conclusion that the channel structure is the important feature in minimizing contact with the water body. It is possible that the process is facilitated by air trapped in the trough regions.

As clearly evident in Figure 2, an array of star-shaped structures is distributed on the wing membrane. These types of structures (termed micrasters) have been previously reported, but their function(s) have remained a mystery.<sup>19,21,22</sup> The micrasters in Figure 2 represent a skeletal framework comprising 5–7 distinct arms consisting of uniformly thin sheets around 90–120 nm in width, many of which originate from the same central location on the star structure and have a secondary nanoroughness on the top ridges (Figure S1). They are typically 5–6  $\mu\text{m}$  in height at the highest point and have a width (extremity of arm to arm distance) generally of 5–6  $\mu\text{m}$ . The center point–center point spacing of structures is  $\sim 10 \mu\text{m}$ .

In order to investigate the interaction of micrasters with water, microdroplets (20–150  $\mu\text{m}$  in diameter) were sprayed onto the wing surfaces. Figure 5A–C shows some of the resulting droplets on the membrane surface. For comparison, droplets of similar volumes were sprayed onto a glass microscope slide and a hydrophobic PDMS surface (Figure 5D,E, respectively).

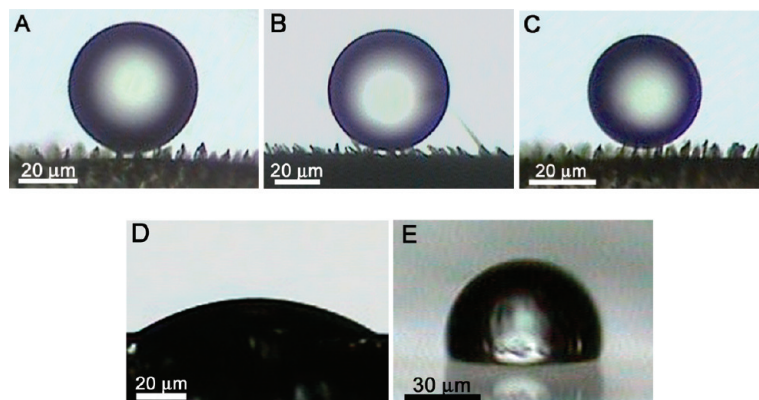


**Figure 5.** Interaction of small micro-sized water droplets with a number of different surfaces. (A,B) Droplets on the termite wing membrane of *Microcerotermes* sp. (45 and 55  $\mu\text{m}$  in diameter, respectively). (C) Droplet on the termite wing membrane of *Nasutitermes* sp. (30  $\mu\text{m}$  in diameter). The droplets maintain their spherical shape and rest on the extremities of the micrasters. For comparison, droplets of similar volumes were also sprayed onto a (D) hydrophilic glass microscope slide and a (E) hydrophobic PDMS surface.

Remarkably, droplets are held above the surface by a number of micrasters *via* contact with their apex facilitating minimal contact with the skeletal sheet arrangement. The microdroplets on the termite wing maintain their spherical shape and occupy regions between the hair arrays (see also Figure S2A,B). The microdroplets interacting with the micrasters show a comparable high equilibrium contact angle to state-of-the-art superhydrophobic surfaces.<sup>23</sup>

A single termite wing may have in excess of one million of these micrasters. It has been postulated that this enormous weight adversely affects termite flight and as a result is slow and erratic.<sup>19</sup> This is thought to increase the likelihood of predation by birds and other animals and restricts dispersal to distant places. In contrary to this hypothesis, we believe these structures not only form an integral component of the anti-wetting hierarchical shielding of the termite but also are in fact designed to significantly minimize weight on the termite wing. If the micrasters seen in Figure 2 were not of a skeletal framework comprising the sheet-like design, but alternatively solid structures comprising microdomes parabolic in shape, then the weight of the wings would increase significantly. Indeed, solid structures of similar dimensions, both natural and man-made, have been reported in the literature and have demonstrated anti-wetting and superhydrophobic properties.<sup>1,24–26</sup> These structures, however, are typically not bound by weight and material constraints.

We can approximate the micrasters as parabolic-shaped sheet structures. If we express the structures having material density ranges at the lower end of insect cuticular material ( $1 \text{ g/cm}^{-3}$ ),<sup>27,28</sup> then the additional weight in relation to the total insect weight would only be 3.2% on *Nasutitermes* sp. and 7.3% on *Microcerotermes* sp. If, however, we approximate the micrasters as solid parabolic three-dimensional domes (a solid fraction represented by a volume with a membrane enclosing the skeletal sheet framework), surprisingly, the weight increase would constitute approximately 37% of the total body mass of *Nasutitermes* sp. and 84% of *Microcerotermes* sp., almost the same weight as that of the insect itself (over 500% of the total wing mass). Thus, the skeletal sheet-like structure arrangement provides anti-wetting support to microdroplets while at the same time minimizing the amount of material and weight required by a significant amount. Weight may be an important factor for the weak flying termites in wet conditions. Termite alates (winged termites) typically have large quantities of stored nutrients but reduce weight by flying with minimal water content and rehydrate during the initial stages of colony foundation.<sup>13,14</sup>

Observations viewed by optical microscopy showed that microdroplets were removed from the membrane surface by at least three mechanisms:

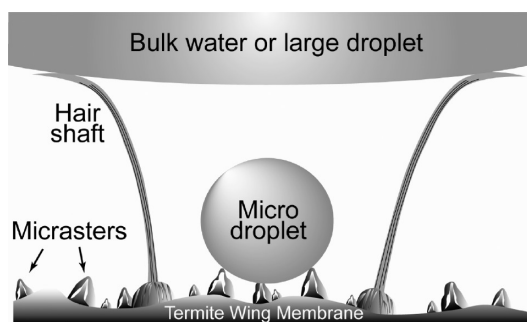


**Figure 6.** Diagrammatic representation of the hierarchical structuring on the termite wing showing macrotrichia and micrasters designed to minimize interaction with water bodies of various sizes. The open sheet architecture on both hair and micraster aides in weight reduction.

- (1) Microdroplets are mobilized by minor vibrations/movements of the wings facilitated by minimal adhesion with the micrasters.
- (2) Larger droplets resting on the hairs absorb microdroplets resting on the micrasters.
- (3) Constant wetting allows microdroplets to build up in size and are then large enough for removal *via* the hair arrays. Droplets as small as  $100 \mu\text{m}$  can be held above the wing surface by the hairs (Figure S3).

Figure 6 shows diagrammatically the anti-wetting scaffolding arrangement on the termite wing. The specialized topographies are designed for minimizing the solid–liquid contact area and maximizing the liquid–air contact. The hair/micraster array demonstrates an elegant hierarchical designed approach for minimizing interaction with water bodies of various length scales. Also, the open membrane hierarchy demonstrates a design for achieving this state utilizing minimal structural material and thus reduced weight for the insect. This feature of multiscale defense architecture may be a common theme for such insects.

The termite will typically encounter droplet conditions when active during storm and wet conditions.<sup>14</sup> Indeed, all of the specimens used in this study were collected during flight in the rain (five separate occasions). This demonstrates that the insects can easily cope with rain where flight has to be maintained. As termites are not typically good fliers and have a low wing flapping rate, the “shedding efficiency” of water on the surface, and thus interaction time with droplets may be critical to maintaining controlled flight.

The evolution of insect wings addresses survival mechanisms. Wing microarchitecture such as hairs allows insects to escape dangerous environments. For example, hairs have been shown to protect green lacewings against spider webs by reducing adhesion.<sup>18</sup> It is possible that the hair array on the termite wings provides a similar defense mechanism for solid–solid contacts. There may be additional functional attributes of the termite hairs; for example, the hairs may help reduce electrostatic interactions with surfaces by increas-

ing the distance between the wing membrane (which constitutes the larger surface area) and the other contacting solid/liquid.

Insects are often threatened by water bodies because of body mass, and so it is not surprising that wing hairs that prevent adhesion to water appear to be an ancestral feature of insect wings.<sup>17</sup> The need to keep wings from sticking to water was apparently solved early in the evolution of winged insects. Such hairs are seen in mayflies and stoneflies.<sup>17,29</sup> Mayflies provide an interesting example for the role of wing hairs. Mayflies are unusual in that they moult twice in the adult form.<sup>30</sup> The subimago stage emerges from the water and makes a single flight to escape the water surface. It has a covering of hairs on the wings. In contrast, the adult stage into which the subimago moults has completely naked wings.<sup>17</sup> It does not contact a body of water because it flies continuously. The presence of the hairs is significant. When wing hairs are removed from mayflies, their ability to escape from a water surface is affected.<sup>30</sup> Mayflies and stoneflies represent early points on different branches (paleopterous vs neopterous) of the main insect radiation,<sup>31</sup> and therefore, either their common ancestor possessed wet-resistant wings or the feature evolved separately, indicating convergent evolution. Hovmöller *et al.*<sup>31</sup> argue that the evidence that extant Palaeoptera are a monophyletic group goes against the theory of aquatic wing origin. Since there are no fossils of the immediate ancestors of winged insects, the pathway for evolution of insect wings is unknown and still dependent on scenarios. Micrasters, however, are absent on the wings of mayflies and stoneflies. This may indicate that, compared to hairs, micrasters evolved more recently as a hydrophobic adaptation. Termites are part of the Dictyoptera and now recognized as being nested within the

cockroaches with *Cryptocercus* as the sister group and mantids as a sister group to the cockroaches.<sup>12</sup> Since *Cryptocercus* are wingless, an investigation of fossil Dictyoptera may enlighten the debate further.

## CONCLUSIONS

The hair array combined with the micraster array demonstrates an elegant hierarchical designed approach for minimizing interaction with water bodies at various length scales. The added resistance to water penetration afforded by the fine architectural structures on the termite aids the insect to interact with a variety of environmental surfaces without becoming immobilized. For example, bulk water bodies (*e.g.*, ponds) and wetted solid surfaces (*e.g.*, leaves) will constitute a hazard. We have observed that termites can escape from a water body even though contact with the water surface is made with the wing by the motion of the insect during takeoff.

Understanding the interaction of water with surfaces (*e.g.*, wetting) through development of the scientific basis for these processes will ultimately lead to the next generation of advanced materials with attributes such as contamination resistance, self-cleaning, and for water collection and conservation.<sup>4,32</sup> This study has also contributed to the understanding of how other insect species (terrestrial and semiaquatic) minimize interactions with water. Furthermore, the progression of micro- and nanostructure formation on insects could aid evolutionary biologists investigating species adaptation to the various environmental conditions, as well as inform the debate on wing evolution. This “free” technology will contribute to the next generation of bioinspired materials and devices for control of fluidic flow, adhesion and wetting properties at the macro- and micro/nanoscales.

## EXPERIMENTAL SECTION

**Photographic and Video Imaging.** Photographs of droplets resting on single excised wings were obtained using a Canon Digital 350D SLR and Canon Ultrasonic EF-S 60 mm macrolens at an 8 megapixel resolution. The photographs were cropped with no further image processing, and scale bars were applied using Photoshop. Videos were captured using a Sony HD video recorder (HDR-CX7) in AVCHD format (MPEG-4 AVC/H.264) and converted from MPEG-2 to .mpg format using Quick Media Converter, v3.6.0. The original resolution of video was  $1440 \times 1080$ .

**Optical Microscopy.** Imaging on single excised termite wings shown in Figures 1C,D, 4, 5, and Figures S2 and S3 in the Supporting Information were obtained using an AIS optical microscope VG8 coupled with a Panasonic color CCTV camera WV-CP410/G attached, allowing image capturing. Top views were captured with the microscope placed in a vertical position, with side views obtained with the microscope in a horizontal position with a  $40\times$  magnification. Data capture was undertaken using Microsoft VidCap32 software. Captured images were imported into Microsoft PowerPoint and converted into TIF format. These were then imported into Photoshop where they were cropped, brightness and contrast were adjusted, and scale bars and labels were applied.

**Scanning Electron Microscopy.** In the case of scanning electron microscope (SEM) imaging, individual hairs attached to AFM probes were placed on an aluminum pin-type stub with carbon-impregnated double-sided adhesive, then sputter coated with 7–10 nm of platinum, before being imaged using a JEOL 6300 field emission SEM at 8 kV. Wing tissues of the termites (approximately  $3 \text{ mm} \times 3 \text{ mm}$ ) were excised and imaged under the same conditions.

**Atomic Force Microscopy.** A TopoMetrix (Veeco Instruments) Explorer TMX-2000 SPM was used to obtain force measurements including hair mechanical properties and adhesion data. This was carried out in the force *versus* distance ( $F-d$ ) mode. A  $130 \times 130 \mu\text{m}^2$  tripod scanner was used with a  $z$  range of  $9.7 \mu\text{m}$ .  $F-d$  curves were acquired at rates of translation in the  $z$  direction in the range of  $2-5 \mu\text{m s}^{-1}$ , with each curve consisting of 600 data points. The analyses were carried out under air-ambient conditions (temperature of  $20-25 \text{ }^\circ\text{C}$  and  $60-75\% \text{ RH}$ ). “Beam-shaped” tipless levers (NT-MDT Ultrasharp) were used for the attachment of hairs and also determination of hair spring constants. The force constants of levers ( $k_N$ ) were determined by accepted methods.<sup>33</sup> The force constants of individual termite hairs were determined by obtaining  $10-20 F-d$  curves on two individual hairs utilizing two tipless beam-shaped levers with similar spring constants ( $k_N$  values of  $0.1 \pm 0.01 \text{ N m}^{-1}$ ). The mea-

measurements were first obtained on the uncoated hair. The same hair was then thinly coated with PDMS, as described in the following section, and  $F-d$  measurements were obtained. Later, a thick layer of PDMS was applied to the hairs, whereby the final  $F-d$  measurements were obtained. The adhesional data were obtained by depositing a 10  $\mu\text{L}$  droplet of Milli-Q water on a slide previously coated with PDMS to ensure a hydrophobic surface. An uncoated termite hair (attached to a lever as described in the section below) was then brought into contact with the droplet (always located *ca.* 500  $\mu\text{m}$  below the top of the drop in order to avoid the meniscus attraction between the hydrophilic lever and the Milli-Q water droplet) and retracted with 10–20  $F-d$  curves obtained. The same hair was then coated in a thin layer of PDMS and finally with a thick layer. The  $F-d$  curves were then analyzed using the TopoMetrix analysis software package (TopoMetrix SPMLab, v 4.0). The values were then entered into SigmaPlot 10.0, whereby standard error values were obtained.

**Hair Attachment and Coating.** Individual termite hairs were scraped off the wing membrane using a surgical scalpel onto clean silicon wafer pieces. These were then placed under an optical microscope. Tipless levers were attached to an in-house positioning translator fixed to an optical microscope which allowed for precise  $x$ ,  $y$ , and  $z$  positioning of the lever. The very end of the lever was first lowered onto the edge of a glue droplet (fast curing Araldite two-part epoxy resin) coating the underside, and then retracted. The lever was then positioned above an individual hair aligned with the long axis of the lever, lowered onto the end of the desired hair, and raised with the hair attached to the end of the lever. The samples were then allowed to dry for 24 h prior to further experimentation. Once the initial measurements were obtained, a mixture of 10:1 base to curing agent of polydimethylsiloxane (PDMS) (Dow Corning, Sylgard-184) was prepared for a thin coating on the hairs. A drop of PDMS was deposited onto a concave microscope slide where the polymer was allowed to spread ( $\sim 1$  min). The slide was then placed under an optical microscope, where a lever with an insect hair attached at the free end was then positioned at the edge of the PDMS droplet and gently lowered ensuring full coverage of the hair, but not the lever itself. The hair was retracted and allowed to cure for a minimum of 48 h under ambient conditions prior to any further experimentation. For a thick coating of PDMS on the hairs, the PDMS mixture placed on the microscope slide was partially cured in the oven for 3 min at 60  $^{\circ}\text{C}$ , and then removed and allowed to cool to room temperature. The sample was then placed under the microscope and the hair dipped  $\sim 5$  times in succession and cured as described above. The layer thickness values for thin coated hair were tens of nanometers, allowing for the microchannels to retain their general shape, and hundreds of nanometers on the thick coated hair. This resulted in thick coated hairs forming smooth cylinders. A similar attachment and coating procedure was applied to measure the spring constants of individual termite hairs, however, with two individual hairs attached to SPM chips to ensure that one end of the hairs remained fixed.

**Acknowledgment.** We acknowledge B. Barlow, S. Hu, and S. Myhra for discussions and suggestions, and thank the reviewers for their helpful comments and suggestions.

**Supporting Information Available:** Three supplementary figures and two supplementary movies. Figure S1 shows an SEM image of the termite wing of *Microcerotermes* sp. Optical images of microdroplets resting between termite wing microtrichia are shown in Figure S2, and a larger droplet being held above the surface of the wing membrane by the microtrichia is shown in Figure S3. Movies 1 and 2 demonstrate how the termite wing resists wetting when a water droplet is forced (or pushed) onto the wing membrane (Movie 1) and dropped onto the wing (Movie 2). This material is available free of charge via the Internet at <http://pubs.acs.org>.

## REFERENCES AND NOTES

- Sun, T.; Feng, L.; Gao, X.; Jiang, L. Bioinspired Surfaces with Special Wettability. *Acc. Chem. Res.* **2005**, *38*, 644–652.
- Yoshimitsu, Z.; Nakajima, A.; Watanabe, T.; Hashimoto, K. Effects of Surface Structure on the Hydrophobicity and Sliding Behavior of Water Droplets. *Langmuir* **2002**, *18*, 5818–5822.
- Huang, T.-L. J.; Ko, J.; Zhu, D.-W.; Fong, B. C. World Patent 99/57185, 2002.
- Holdgate, M. W. The Wetting of Insect Cuticles by Water. *J. Exp. Biol.* **1955**, *32*, 591–617.
- Wagner, P.; Neinhuis, C.; Barthlott, W. Wettability and Contaminability of Insect Wings as a Function of their Surface Sculptures. *Acta Zoologica* **1996**, *77*, 213–225.
- Cong, Q.; Chen, G.-H.; Fang, Y.; Ren, L.-Q. Study on the Super-Hydrophobic Characteristic of Butterfly Wing Surface. *J. Bionics Eng.* **2004**, *1*, 249–255.
- Gorb, S. N.; Kesel, A.; Berger, J. Microsculpture of the Wing Surface in Odonata: Evidence for Cuticular Wax Covering. *Arthropod Struct. Dev.* **2000**, *29*, 129–135.
- Gao, X.; Jiang, L. Water-Repellent Legs of Water Striders. *Nature* **2004**, *432*, 36.
- Parker, A. R.; Lawrence, C. R. Water Capture by a Desert Beetle. *Nature* **2001**, *414*, 33–34.
- Parker, A. R.; Townley, H. E. Biomimetics of Photonic Nanostructures. *Nat. Nanotechnol.* **2007**, *2*, 347–353.
- Watson, G. S.; Myhra, S.; Cribb, B. W.; Watson, J. A. Putative Function(s) and Functional Efficiency of Ordered Cuticular Nano-Arrays on Insect Wings. *Biophys. J.* **2008**, *94*, 3352–3360.
- Inward, D.; Beccaloni, G.; Eggleton, P. Death of an Order: A Comprehensive Molecular Phylogenetic Study Confirms That Termites Are Eusocial Cockroaches. *Biol. Lett.* **2007**, *3*, 331–335.
- Nalepa, C. A.; Miller, L. R.; Lenz, M. Flight Characteristics of *Mastotermes darwiniensis* (Isoptera, Mastotermitidae). *Insectes Soc.* **2001**, *48*, 144–148.
- The Insects of Australia: A Textbook for Students and Research Workers*; Melbourne University Press: Carlton, Victoria, 1991; Vol. 1.
- Pearce, M. J. *Termites Biology and Pest Management*; CAB International: UK, 1997; p 172.
- Gorb, S. *Attachment Devices of Insect Cuticle*; Kluwer Academic Publishers: New York, 2001; pp 21–36.
- Marden, J. H.; Kramer, M. G. Surface-Skimming Stoneflies: A Possible Intermediate Stage in Insect Flight Evolution. *Science* **1994**, *266*, 427–430.
- Masters, W. M.; Eisner, T. The Escape Strategy of Green Lacewings from Orb Webs. *J. Insect Behav.* **1990**, *3*, 143–157.
- Roonwal, M. L. Wing Microsculpturing in Termites (Isoptera) under the Scanning Electron Microscope. *Zool. Anz. Jena* **1985**, *215*, 219–230.
- Feng, X.-Q.; Gao, X.; Wu, Z.; Jiang, L.; Zheng, Q.-S. Superior Water Repellency of Water Strider Legs with Hierarchical Structures: Experiments and Analysis. *Langmuir* **2007**, *23*, 4892–4896.
- Rathore, N. S. Third Study of Evolution and Systematic Significance of Wing Micro-Sculpturing in Termites. Micrasters in Some Thinotermitidae and Termitidae. *Zool. Anz.* **1977**, *198*, 298–312.
- Rathore, N. S. On a New Systematic Character in Termites, the Microsters. *Z. Zool. Syst. Evol. Berlin* **1974**, *12*, 55–76.
- Woodward, I. S.; Schofield, W. C. E.; Roucoules, V.; Badyal, J. P. S. Super-Hydrophobic Surfaces Produced by Plasma Fluorination of Polybutadiene Films. *Langmuir* **2003**, *19*, 3432–3438.
- Sun, M.; Luo, C.; Xu, L.; Ji, H.; Ouyang, Q.; Yu, D.; Chen, Y. Artificial Lotus Leaf by Nanocasting. *Langmuir* **2005**, *21*, 8978–8981.
- Ma, M.; Hill, R. M. Superhydrophobic Surfaces. *Curr. Opin. Colloid Interface Sci.* **2006**, *11*, 193–202.
- Nosonovsky, M.; Bhushan, B. Biologically Inspired Surfaces: Broadening the Scope of Roughness. *Adv. Funct. Mater.* **2008**, *18*, 843–855.
- Lockey, K. H. The Thickness of Some Insect Epicuticular Wax Layers. *J. Exp. Biol.* **1960**, *37*, 316–329.

28. Neville, A. C.; Parry, D. A. D.; Woodhead-Galloway, J. The Chitin Crystallite in Arthropod Cuticle. *J. Cell Sci.* **1976**, *21*, 73–82.
29. Marden, J. H.; O'Donnell, B. C.; Thomas, M. A.; Bye, J. Y. Surface-Skimming Stoneflies and Mayflies: The Taxonomic and Mechanical Diversity of Two-Dimensional Aerodynamic Locomotion. *Phys. Biochem. Zool.* **2000**, *73*, 751–764.
30. Edmunds, G. F., Jr.; McCafferty, W. P. The Mayfly Subimago. *Annu. Rev. Entomol.* **1988**, *33*, 509–529.
31. Hovmöller, R.; Pape, T.; Källersjö, M. The Palaeoptera Problem: Basal Pterygote Phylogeny Inferred from 18S and 28S rDNA Sequences. *Cladistics* **2002**, *18*, 313–323.
32. Bergeron, V.; Quéré, D. Physicsweb, Physics World, May, 2001.
33. Cleveland, J. P.; Manne, S.; Bocek, D.; Hansma, P. K. A Non-Destructive Method for Determining the Spring Constant of Cantilevers for Scanning Force Microscopy. *Rev. Sci. Instrum.* **1993**, *64*, 403–405.